NANOSYSTEMS: PHYSICS, CHEMISTRY, MATHEMATICS, 2014, 5 (6), P. 803–810

# SPECTRAL REGULARITIES OF THE CRITICAL ENERGY DENSITY OF THE PENTAERYTHRIOL TETRANITRATE -ALUMINUM NANOSYSTEMS INITIATED BY THE LASER PULSE

A. V. Kalenskii, M. V. Ananyeva

Kemerovo state University, Kemerovo, 650043, Russia

kriger@kemsu.ru

**PACS 42.25.Gy, 82.33.Vx**

In this work, the absorption of aluminum nanoparticles and the critical energy densities of the pentaerythritol tetranitrate -aluminum nanosystems, initiated by laser pulses, were calculated for wavelengths from 400 to 1200 nm. Data showed that it is necessary to consider both thermal and optical characteristics in order to calculate the critical initiation energy density and the radius of the most dangerous inclusion. The nanoparticle's radius, corresponding to the maximum on the curve of absorptivities, and the maximum's amplitude and critical energy density of the explosive materials, were all shown to depend on the initiating wavelength. The maximum of the aluminum nanoparticles' absorptivity and minimum of the critical energy density of the explosive decomposition were observed for the 400 nm wavelength, there is also a local maximum at 850 nm. The results from the experiment qualitatively and quantitatively agree with our calculations. These results are very important to optimize the cap composition for the optical detonators.

**Keywords:** Hot spot model, laser initiation, metal nanoparticles absorption, pentaerythritol tetranitrate.

*Received: 10 November 2014*

## 1. Introduction

The process of discovering energetic materials which have selective sensitivity to laser irradiation, in order to determine the ideal cap compositions for optical detonators has been carried out for almost 20 years. The first optical detonators were based on silver and lead azides. Their disadvantages were the high sensitivity not only to the laser impulse but also to the stroke, friction and heating. Because of their low selectivity, optical detonators based on priming powder were not widely adopted. The main direction of current research is now based on composite materials consisting of explosive materials and photosensitive metal particles [1-3]. The initiation threshold values for composites of pentaerythritol tetranitrate (PETN) and aluminum nanoparticles were obtained. Sensibility to laser initiation for these composites was shown to be about 1 J/cm$^2$, while their sensibility to striking remained the same [1-4]. This proves both the possibility of using disruptive explosives, containing metal nanoparticles, as a cup of the optical detonators, and the role of the metal nanoparticles as the centers for light absorption in the bulk matrix of the transparent media. To find the ideal material, optimal sizes for the metal inclusions and parameters for the initiating system, it is necessary to consider several factors, which used to be considered negligible: the dependence of the metal nanoparticles' absorption on their sizes and the initiation wavelength. The aim of this work is to theoretically estimate the aluminum nanoparticles' absorption in the PETN matrix for the initiating wavelengths from 400 to 1200 nm; calculation of the minimal values

of the critical energy density for PETN – aluminum composites for different inclusion sizes and initiating wavelengths.

## 2. Hot spot model

The hot spot model [1-4] is based on the assumption that in the matrix of the energetic material there are nanoparticles, which can absorb irradiation very efficiently. In this model, it is assumed that the main result of light absorption is the heating of these particles. The heating causes growth of the surrounding energetic material's temperature and formation of the center of the self-accelerating exothermic reaction. The system of equations, describing conductive heat-transfer processes in the nanoparticles and media and the exothermal decomposition in case of the spherical symmetry, are [2-5]:

$$\begin{aligned}
&\frac{\partial T}{\partial t} = \alpha \cdot \left( \frac{\partial^2 T}{\partial x^2} + \frac{2}{x} \cdot \frac{\partial T}{\partial x} \right) + \frac{Q}{c} k_0 n \cdot \exp\left( -\frac{E}{k_B T} \right), \quad x > R, \\
&\frac{\partial n}{\partial t} = -k_0 n \cdot \exp\left( -\frac{E}{k_B T} \right), \qquad x > R, \\
&\frac{\partial T}{\partial t} = \alpha_M \cdot \left( \frac{\partial^2 T}{\partial x^2} + \frac{2}{x} \cdot \frac{\partial T}{\partial x} \right), \qquad x < R,
\end{aligned} \tag{1}$$

where $T$ – temperature, $n$ – relative concentration of the explosive material (PETN), which decreases during the reaction from 1 to 0, $\alpha$ and $\alpha_M$ – are the coefficients of thermal conductivity of the matrix and inclusion materials, $R$ is the inclusion radius, $k_B$ – Boltzmann constant, $E$ – energy of activation, $Q$ – heat efficiency of the decomposition, $k_0$ – preexponential factor, $c$ is the volumetric heat capacity of the matrix. The boundary conditions for $x = R$ are:

$$J - c_M \alpha_M \cdot \left. \frac{\partial T}{\partial x} \right|_{x \to R-0} + c\alpha \cdot \left. \frac{\partial T}{\partial x} \right|_{x \to R+0} = 0, \tag{2}$$

where $c_M$ is the volumetric heat capacity of the nanoparticle, $J(t)$ – is the absorbed density of the laser pulse radiation power. During the calculations the following parameters were used (the same as in works [2-5]): $= 2.22$ J/(cm$^3$K), $c_M$= 2.7 J/(cm$^3$K), $= 165$ kJ/(mole·K), $k_0$= 1.210$^{16}$ s$^{-1}$, $\alpha$=1.1·10$^{-3}$ cm$^2$s$^{-1}$, $\alpha_M$= 0.97 cm$^2$s$^{-1}$, $Q$ = 9.64 kJ/cm$^3$.

To research the explosive decomposition of energetic materials, the Nd:Yag based laser system is often used [6-7]. The dependence of the laser's radiating power on time is close to the function of the normal distribution [7-8]. Taking as a zero-time the moment of the impulse's maximum, one can obtain for $J(t)$ the following equation [9-10]:

$$J(t) = \sqrt{\pi} \cdot \mathrm{Q_{abs}} R^2 k_i H_0 \cdot \exp\left( -k_i^2 t^2 \right), \tag{3}$$

where $k_i = 8.325 \cdot 10^7$ c$^{-1}$ – parameter, determining the impulse duration (corresponds to the impulse duration on the half-height 20 ns); $\mathrm{H_0}$ – impulse energy density; $\mathrm{Q}_{abs}$ – the coefficient of absorption efficiency equal to the ratio of intensities of radiation absorbed and incident on the inclusion. The value of $\mathrm{Q}_{abs}$ depends on different factors – the inclusion radius and material of inclusion, and radiation wavelength. Multipliers of Eq. (3) normalize the integral of J(t) over time by $\mathrm{H_0}$.

$\mathrm{Q}_{abs}$ of the spherical inclusion was calculated in terms of Mie theory. According to this theory, $\mathrm{Q}_{abs}$ might be calculated as a difference between coefficients of extinction ($Q$)

and the scattering coefficient ($Q_{sca}$) ($Q_{abs}$ = $Q$ - $Q_{sca}$) [11]:

$$Q_{sca} = \frac{2}{\rho^2}\sum_{l=1}^{\infty}(2l+1)\cdot\left(|c_l|^2+|b_l|^2\right), Q = \frac{2}{\rho^2}Im\sum_{l=1}^{\infty}(2l+1)\cdot(c_l-b_l), \tag{4}$$

where $\rho = 2\pi R m_0/\lambda$, $m_0$=1.54 [12] – PETN's refractive index. $c_1$ and $b_1$ coefficients, which can be obtained using the boundary conditions for the nanoinclusion's surface [11-12]:

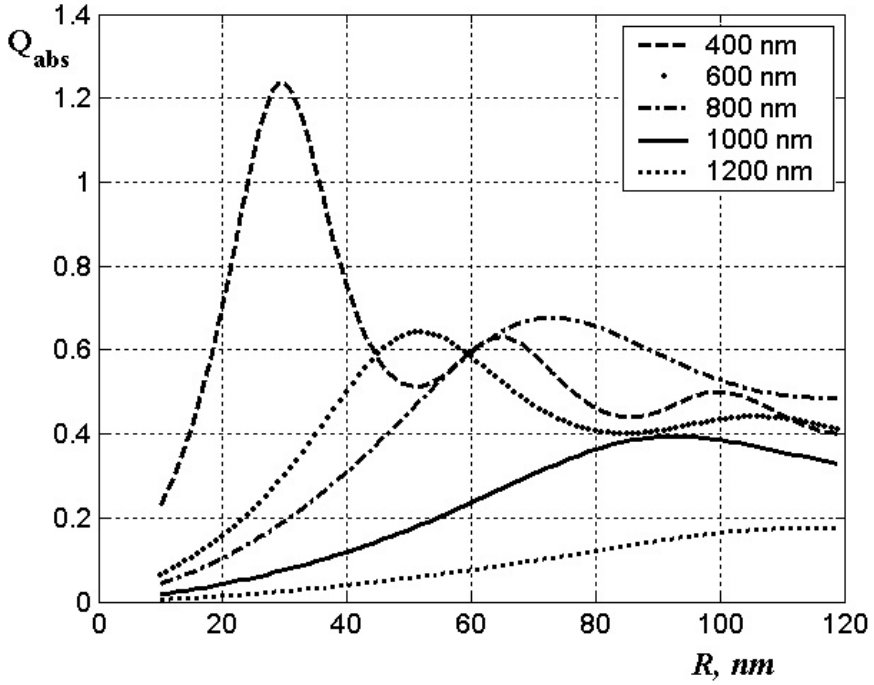


FIG. 1. Calculated dependences of the aluminium nanoparticles' absorptivity ($Q_{abs}$) in PETN-matrix on the particles' sizes for wavelengths 400, 600, 800, 1000, 1200 nm

$$c_l = i\frac{\psi_l(\rho)\psi_l'(n\rho) - n\psi_l'(\rho)\psi_l(n\rho)}{\zeta_l(\rho)\psi_l'(n\rho) - n\zeta_l'(\rho)\psi_l(n\rho)},$$

$$b_l = -i\frac{\psi_l'(\rho)\psi_l(n\rho) - n\psi_l(\rho)\psi_l'(n\rho)}{\zeta_l'(\rho)\psi_l(n\rho) - n\zeta_l(\rho)\psi_l'(n\rho)}, \tag{5}$$

where $n$=$m_i/m_0$ – complex refractive index of the nanoparticle relative to the matrix. To calculate the functions ($\psi_l$ and $\zeta_l$) and their derivatives ($\psi_l'$ and $\zeta_l'$) the following recurrence relations were used:

$$\psi_{l+1}(z) = \frac{2l+1}{z}\psi_l(z) - \psi_{l-1}(z), \tag{6}$$

$$\psi_l'(z) = \psi_{l-1}(z) - \frac{l}{z}\psi_l(z). \tag{7}$$

If $l = 1; 2$ the special functions are:

$$\psi_0(z) = \sin z \qquad \psi_1(z) = \frac{\sin z}{z} - \cos z, \tag{8}$$

$$\zeta_0(z) = ie^{-iz} \qquad \zeta_1(z) = -e^{-iz}(1 - i/z). \tag{9}$$

The use of recurrence relations (6-9) greatly shortened the time required for calculation. Dependences of the aluminum nanoparticles' absorptivity in the PETN-matrix on the particles' sizes, calculated using equation (4-9) are presented in fig. 1. Calculations were done for different initiating wavelengths – 400, 600, 800, 1000, and 1200 nm. Each dependence has a maximum ($Q_{abs\ max}$), its position ($R_{max}$) depending on the irradiation wavelength. For smaller radii, the curve decreases to zero, and in the extreme case $R \to 0$, the dependence changes according to Rayleigh–Jeans law. For nanoparticles having larger radii, the curve plateaus with some oscillations. In terms of the Mie theory, the wavelength influences the $Q_{abs}$ because the factorial expansion arguments of the special functions are $\rho = 2\pi R m_0/\lambda$ and $m_i\rho/m_0$. If $m_i$ did not depend on the wavelength, the $Q_{abs}(\rho)$ dependences would coincide. The real and imaginary parts of $m_i$ change considerably over the range of the examined wavelengths (Table 1). Table 1 shows the following: complex refractive index of aluminum [13], the calculated radii of aluminum particles having the largest absorptivity and those absorptivity values. The results presented for the wavelengths from 400 to 1200 nm, for which the complex refractive index of aluminum are well known [13-14], and for wavelengths of 1064 and 532 nm – the first and the second harmonic of the Nd:YAG laser using in the experimental work [2-3]. If the wavelength increases, the absorptivity maximum moves to the area of the larger radii (fig. 1), the maximum's amplitude – decreases (fig. 2). But for $\lambda$ =850 nm there is a local maximum, caused by the local maxima of the real and imaginary parts of the complex refractive index. Thus, for the $Q_{abs\ max}(\lambda)$ dependence for aluminum in a PETN-matrix, there is a local maximum, and so, there must be corresponding minimum of critical initiation energy for explosive decomposition. The calculated $Q_{abs\ max}(\lambda)$ dependence over wavelengths ranging from 400–1200 nm is presented on fig. 2.

In order to calculate the critical parameters for explosive decomposition, a numerical solution for models (1)–(3) was made using a variable-pitch grid. A step in the vicinity of the inclusions with the radii $R \geqslant 30$ nm was no more than 1/20 of the thickness of the inert substance heated during the pulse ($\sqrt{2\alpha/k_i}$), then the cell size increased exponentially, so that the total thickness of the surrounding material was no less than 7R. For a half-height pulse duration of 20 ns, the heating length was equal to ≈50 nm and the size of cells near the inclusion was about 2.5 nm. The step of the grid inside the inclusion exceeded the step outside by $\sqrt{\alpha_M/\alpha}$ times. The cell on the bound inclusion-matrix contained both the matrix material and the inclusion material with the thickness equal to the half step of the grid. For the mentioned characteristics, the size of the cell inside the inclusion was about 10 nm, which is approximately the thickness of the light absorption layer. This layer does not exceed 10 nm for most metals. This method allows one to make a reasonable consideration of light absorption by means of boundary conditions (2) [15].

The ordinary differential equation set obtained after dividing the space into cells was solved by the Runge — Kutta method of 1–5 orders with a variable time step. A relative error at an integration step does not exceed $10^{-9}$, whereas the integral relative error estimated by the precision of performance of the law of conservation of energy did not exceed $2.5 \cdot 10^{-5}$.

Calculation of the radius of the most dangerous inclusion was made using the following method. First the absorptivities for the different particles' radii were calculated. Then, the critical energy density was calculated for these radii in terms of models (1-3). Next, quadratic

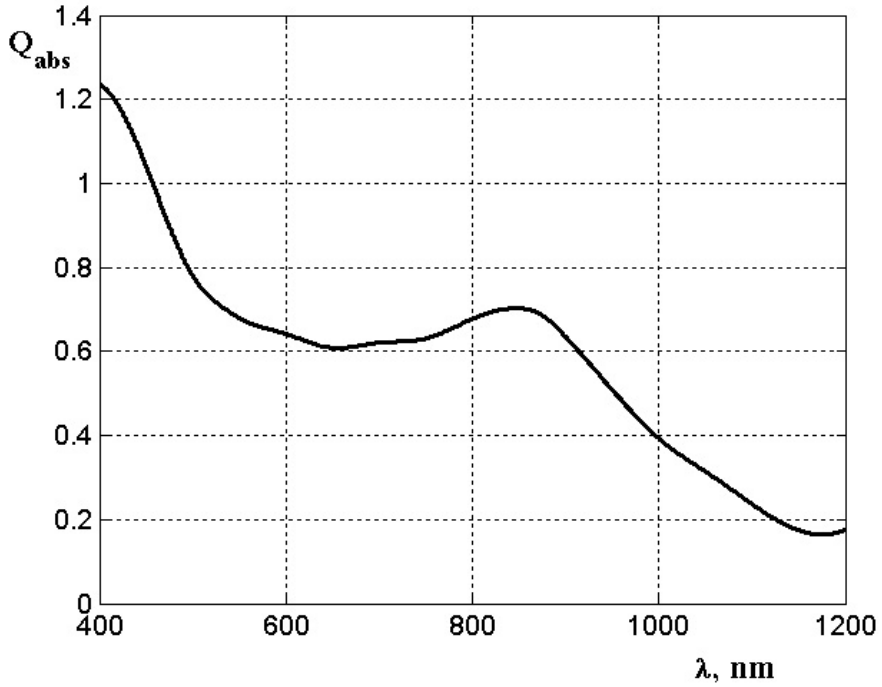


FIG. 2. Dependences of the aluminum nanoparticles' maximal absorptivity in PETN matrix on the initiating wavelength in a spectral range 400 – 1200 nm

interpolation was done to obtain the minimal value results. After that, the critical energy density was calculated at the point of this minimum. All these steps were repeated until the most dangerous inclusion's radius accuracy became 0.1 nm.

Fig. 3 shows dependences of the critical energy density on the radius of the aluminum inclusion in the PETN-matrix for initiating wavelengths of 532, 700, 850, 900, and 1064 nm. For each wavelength, there is an optimum radius of the nanoparticle ($R_c$), which corresponds to the minimum critical energy density ($H_c$), for the definite impulse duration. Values $R_c$ and $R_{max}$ for each wavelength have some differences (see table), this is due to the particularities of the nanoparticle heating by the laser pulse in solid-state matrix. For 20 ns pulse duration, there is a size of the nanoparticles, which is heated to the maximum temperature (particularities of the absorption were not considered – $Q_{abs} = 1$). The absorption cross section of the particle is $\pi R^2$, heat capacity of the system nanoparticle – matrix layer might be written as $\frac{4\pi}{3} \cdot \left( c_M R^3 + c \left( \left( R + \sqrt{2\alpha/k_i} \right)^3 - R^3 \right) \right)$ [11], where $h \approx \sqrt{2\alpha/k_i}$ – thickness of the energetic material's layer, which is heated during the laser action. Therefore, the dependence of the heat rate ($\Delta$T) of the particle on the nanoparticle's sizes during the pulse action is:

$$\Delta T = \frac{HR/4c}{R\xi_1\sqrt{2\alpha/k_i} + \xi_1^2 \cdot 2\alpha/k_i + c_M R^2/3c}, \tag{10}$$

where $\xi_1$ – variable parameter, its value is about 1 [11].

TABLE 1. Calculated parameters for the absorption and explosive decomposition process of the aluminum-PETN composites – complex refractive index ($m_i$), maximum of absorptivity ($Q_{abs\ max}$) and particle's radius $R_{max}$ corresponding to this maximum, minimum of critical energy density ($H_c$), optimal particle's radius $R_c$

| $\lambda$, nm | $m_i$ | $Q_{abs\ max}$ | $R_{max}$, nm | $H_c$, $\mu$J/cm$^2$ | $R_c$, nm |
|---|---|---|---|---|---|
| 400 | 0.32-3.72i | 1.2358 | 30 | 7.25 | 30.7 |
| 450 | 0.41-4.06i | 1.0410 | 35 | 7.93 | 36.1 |
| 500 | 0.5-4.59i | 0.7815 | 41 | 9.93 | 42.1 |
| 532 | 0.56-4.86i | 0.7064 | 44 | 10.66 | 45.8 |
| 550 | 0.6-5.01i | 0.6799 | 46 | 10.93 | 47.6 |
| 600 | 0.77-5.46i | 0.6419 | 52 | 11.25 | 53.1 |
| 650 | 0.98-5.97i | 0.6090 | 57 | 11.59 | 58.6 |
| 700 | 1.26-6.4i | 0.6210 | 63 | 11.22 | 63.8 |
| 750 | 1.5-6.72i | 0.6307 | 68 | 10.95 | 68.8 |
| 800 | 1.78-6.87i | 0.6771 | 73 | 10.16 | 73.5 |
| 850 | 1.91-6.9i | 0.7027 | 78 | 9.77 | 77.7 |
| 875 | 1.82-6.87i | 0.6871 | 80 | 9.99 | 79.7 |
| 900 | 1.7-6.97i | 0.6364 | 82 | 10.79 | 81.8 |
| 950 | 1.4-7.22i | 0.51 | 87 | 13.52 | 86.6 |
| 1000 | 1.17-7.58i | 0.3939 | 93 | 17.58 | 92.1 |
| 1064 | 0.98-8.03i | 0.2942 | 100 | 23.66 | 98.7 |
| 1100 | 0.85-8.33i | 0.2375 | 104 | 29.43 | 102.2 |
| 1200 | 0.78-9.16i | 0.1757 | 115 | 40.48 | 111.6 |

Maximum of the dependence corresponds to the $R_m = \xi_1\sqrt{3c/c_M} \cdot \sqrt{2\alpha/k_i}$. The existence of the optimal nanoparticle's size for which the heating rate is maximal was postulated in previous works. If the half-height pulse duration is 20 ns, then $R_m$=75 nm. Table 1 shows the calculated minimum energy densities for the explosive decomposition of aluminum-PETN composites, optimal radius with the minimal initiating energy density for the laser wavelengths from 400 to 1200 nm. If $\lambda \leqslant$800 nm, the radius, corresponding to the absorptivity maximum, $R_{max} < R_m$ (75 nm), and so the optimal radius, corresponding to the minimal critical energy density, $R_c > R_{max}$, i.e. the optimal radius for explosive decomposition initiation is larger than the radius, corresponding to the absorptivity maximum. If $\lambda \geqslant$850 nm $R_{max} > R_m$, and so the optimal radius of the particle is smaller than the radius, corresponding to the maximum of absorptivity. Calculated critical energy densities are minimal if $\lambda = 400$ nm and have local minimum at $\lambda = 850$ nm. Minimal critical energy densities for the first harmonic of the Nd:YAG laser in 2.2 times bigger than the same values for the second harmonic. This fact is in good agreement with the experimental data (for the first harmonic – 1.15 J/cm$^2$, for the second – 0.7 J/cm$^2$ [3]), where this difference is 1.6.

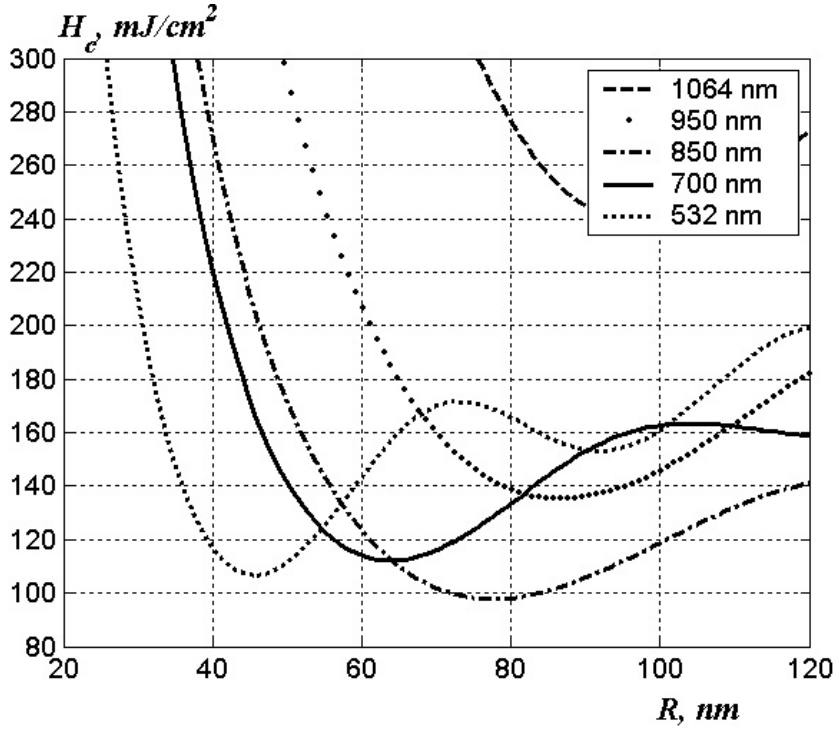


FIG. 3. Dependences of the critical energy density on the aluminum nanoparticle's radius in PETN matrix for the initiating wavelengths 532, 700, 850, 900 and 1064 nm

## 3. Conclusion

In this work, the dependences of the absorption of the aluminum nanoparticles and the critical energy densities of the pentaerythritol tetranitrate-aluminum composites were calculated for the wavelengths from 400 nm to 1200 nm. It was shown that it is necessary to consider both thermal and optical characteristics in order to calculate the critical initiation energy density and the radius of the most dangerous inclusion. The nanoparticle's radius, corresponding to the maximum on the curve of absorptivities, the maximum's amplitude and critical energy density of the explosive materials, were all shown to be dependent upon the initiating wavelength. The maximum of the aluminum nanoparticles' absorptivity and minimum of its critical energy density of the explosive decomposition are observed for the 400 nm wavelength, there is also a local maximum at the 850 nm wavelength. The results of the experiment qualitatively and quantitatively agree with our calculations. These results are necessary to determine the ideal cap composition for optical detonators.

## Acknowledgments

This work was supported by Ministry of Education and Science of the Russian Federation (governmental project No. 2014/64) and Russian Foundation for Basic Research for the financial support (grant 14-03-00534 ).

## References


[1] Chumakov Yu.A., Knyazeva A.G. Initiation of reaction in the vicinity of a single particle heated by microwave radiation. *Fizika goreniya i vzryva*, **48**(2), P. 24–30 (2012).

[2] Ananyeva M.V., Zvekov A.A., et al. Promising compounds for the cap of optical detonator. *Perspektivnye materialy*, **7**, P. 5–12 (2014).

[3] Aduev B.P., Nurmukhametov D.R., et al. Vzryvchatoye razlozheniye TENa s nanodobavkami alyuminiya pri vozdeystvii impulsnogo lazernogo izlucheniya razlichnoy dliny volny. *Khimicheskaya fizika*, **32**(8), P. 39–42 (2013).

[4] Kalenskii A.V., Zvekov A.A., et al. Influence of the laser irradiation wavelength on the energetic materials' initiation critical energy. *Fizika goreniya i vzryva*, **50**(3), P. 98–104 (2014).

[5] Kalenskii A.V., Ananyeva M.V., Zvekov A.A., Zykov I.Yu. Spectrum dependence of the critical energy density of composites based on pentaerythritol tetranitrate with nikel nanoparticles. *Fundamental'nye problemy sovremennogo materialovedenia*, **11**(3), P. 340–345 (2014).

[6] Kriger V.G., Kalenskii A.V., et al. Opredelenie shiriny fronta volny reakcii vzryvnogo razlozhenija azida serebra. *Fizika goreniya i vzryva*, **48**(4), P. 129–136 (2012).

[7] Korepanov V.I., Lisicyn V.M., Oleshko V.I., Cipilev V.P. K voprosu o kinetike i mehanizme vzryvnogo razlozhenija azidov tjazhelyh metallov. *Fizika goreniya i vzryva*, **42**(1), P. 106–119 (2006).

[8] Aduev B.P., Nurmuhametov D.R., Cipilev V.P., Furega R.I. Vlijanie dobavok ul"tradispersnyh chastic al-c na chuvstvitel"nost" tjena k lazernomu vozdejstviju. *Fizika goreniya i vzryva*, **49**(2), P. 102–105 (2013).

[9] Kriger V.G., Kalenskii A.V., Ananyeva M.V., Borovikova A.P. Critical initiation-energy density as a function of single-crystal size in explosive decomposition of silver azide. *Fizika goreniya i vzryva*, **44**(2), P. 76–78 (2008).

[10] Aduev B.P., Ananyeva M.V., et al. Mikroochagovaja model' lazernogo iniciirovanija vzryvnogo razlozhenija jenergeticheskih materialov s uchetom plavlenija. *Fizika goreniya i vzryva*, **50**(6), P. 92–99 (2014).

[11] Kriger V.G., Kalenskii A.V., et al. Vliyaniye effektivnosti pogloshcheniya lazernogo izlucheniya na temperaturu razogreva vklyucheniya v prozrachnykh sredakh. *Fizika goreniya i vzryva*, **48**(6), P. 54–58 (2012).

[12] Nikitin A.P. Raschet kriticheskih parametrov iniciirovanija teplovogo vzryva tjena s nanochasticami medi na raznyh dlinah voln. *Mezhdunarodnoe nauchnoe izdanie Sovremennye fundamental'nye i prikladnye issledovanija*, **4**(11), P. 68–75 (2013).

[13] Zolotarev V.M., Morozov V.N., Smirnova E.V. *Opticheskie postojannye prirodnyh i tehnicheskih sred.* L.: Himija, 216 p. (1984).

[14] Aduev B.P., Nurmukhametov D.R., et al. Integrating Sphere Study of the Optical Properties of Aluminum Nanoparticles in Tetranitropentaerytrite. *Zhurnal Tekhnicheskoi Fiziki*, **84**(9), P. 126–131 (2014).

[15] Kriger V.G., Kalenskii A.V., Zvekov A.A., Zykov I.Yu., Nikitin A.P. Protsessy teploperenosa pri lazernom razogreve vklyucheny v inertnoy matritse. *Teplofizika i aeromekhanika*, **20**(3), P. 375–382 (2013).

[16] Aleksandrov E. I., Cipilev V. P. Issledovanie vlijanija dlitel'nosti vozbuzhdajushhego impul'sa na chuvstvitel'nost' azida svinca k dejstviju lazernogo izluchenija. *Fizika goreniya i vzryva*, **20**(6), P. 104–108 (1984).

[17] Burkina R.S., Morozova E.Ju., Cipilev V.P. Iniciirovanie reakcionno-sposobnogo veshhestva potokom izluchenija pri pogloshhenii ego neodnorodnostjami veshhestva. *Fizika goreniya i vzryva*, **47**(5), P. 95–105 (2011).